Permeation of Na^+ Through Open and Zn^{2+}-Occupied Conductance States of Cardiac Sodium Channels Modified by Batrachotoxin: Exploring Ion-Ion Interactions in a Multi-Ion Channel

Laurent Schild* and Edward Moczydlowski‡

*Institut de Pharmacologie, de l'Universite de Lausanne, rue du Bugnon 27, CH-1005, Lausanne, Switzerland; ‡Department of Pharmacology and Department of Cellular and Molecular Physiology, Yale University School of Medicine, New Haven, Connecticut 06510 USA

ABSTRACT Mammalian heart sodium channels inserted into planar bilayers exhibit a distinctive subconductance state when single batrachotoxin-modified channels are exposed to external Zn^{2+}. The current-voltage behavior of the open state and the Zn^{2+}-induced substate was characterized in the presence of symmetrical Na^+ ranging from 2 to 3000 mM. The unitary conductance of the open state follows a biphasic dependence on [Na^+] that can be accounted for by a 3-barrier-2-site model of Na^+ permeation that includes double occupancy and Na^+-Na^+ repulsion. The unitary conductance of the Zn^{2+} substate follows a monophasic dependence on [Na^+] that can be explained by a similar 3-barrier-2-site model with low affinity for Na^+ and single occupancy due to repulsive interaction with a Zn^{2+} ion bound near the external entrance to the pore. The apparent association rate of Zn^{2+} derived from dwell-time analysis of flickering events is strongly reduced as [Na^+] is raised from 50 to 500 mM. The apparent dissociation rate of Zn^{2+} is also enhanced as [Na^+] is increased. While not excluding surface charge effects, such behavior is consistent with two types of ion-ion interactions: 1) A competitive binding interaction between Zn^{2+} and Na^+ due to mutual competition for high affinity sites in close proximity. 2) A noncompetitive, destabilizing interaction resulting from simultaneous occupancy by Zn^{2+} and Na^+. The repulsive influence of Zn^{2+} on Na^+ binding in the cardiac Na^+ channel is similar to that which has been proposed to occur between Ca^{2+} and Na^+ in structurally related calcium channels. Based on recent mutagenesis data, a schematic model of functionally important residues in the external cation binding sites of calcium channels and cardiac sodium channels is proposed. In this model, the Zn^{2+}-induced subconductance state results from Zn^{2+} binding to a site in the external vestibule that is close to the entrance of the pore but does not occlude it.

INTRODUCTION

Voltage-dependent channels selective for Na^+ and Ca^{2+} are structurally related membrane proteins that consist of four internally homologous domains I–IV (Numa and Noda, 1986; Tanabe et al., 1987). Molecular details related to the mechanism of ion conduction through these two channels have perceptibly begun to emerge with the identification of sodium channel mutations that affect permeation. This progress began with the finding that mutation of glutamate 387 to glutamine in the external S5–S6 linker region of domain I of rat brain sodium channel II virtually abolished sensitivity to the mutually competitive toxin blockers, tetrodotoxin (TTX) and saxitoxin (STX) (Noda et al., 1989). Since it was suspected that the TTX/STX site is associated with the external vestibule of the channel (Hille, 1975), it seemed probable that residues affecting the binding affinity for these toxins may be close to the channel entrance. This hypothesis was verified by mutational analysis of residues near glutamate 387 in the primary sequence and homologous positions in domains II–IV, which identified additional sites that simultaneously affected unitary conductance and toxin block (Terlau et al., 1991). Comparison of sequence homology in this region between sodium channels and calcium channels further led to the identification of a critical position in the sequence alignment that controls selectivity for monovalent and divalent inorganic cations (Heinemann et al., 1992b). This unique position contains four glutamate residues in domains I–IV of calcium channels and has aspartate (I), glutamate (II), lysine (III), and alanine (IV) residues in the respective I–IV homologous domains of sodium channels.

Additional support for association of the S5–S6 linker region with the conducting pore is based on evidence that a unique cysteine residue (Cys^{374}) in domain I of the rat cardiac sodium channel is primarily responsible for the distinctive low affinity of this sodium channel isoform for TTX/STX and the high affinity for block by Cd^{2+} and Zn^{2+}. Planar bilayer experiments (Schild and Moczydlowski, 1991) and [^{3}H]STX binding experiments with cardiac sodium channels (Doyle et al., 1993) have shown that Zn^{2+} and Cd^{2+} competitively inhibit binding of STX with a K_D similar to that for their own blocking reaction. These results suggest that an externally accessible site that mediates high affinity block by Zn^{2+} and Cd^{2+} in cardiac sodium channels (Ravindran et al., 1991) is an overlapping subsite of the STX binding site. Chemical modification experiments have also implicated a sulfhydryl group in the high affinity binding site for Zn^{2+} and STX (Schild and Moczydlowski, 1991; Doyle et al., 1993). Mutation of the suspected cysteine 373 residue in the heart sodium channel to tyrosine found in the muscle

Received for publication 26 August 1993 and in final form 10 December 1993.

Address reprint requests to Edward Moczydlowski, Department of Pharmacology, Yale University School of Medicine, 333 Cedar St., New Haven, CT 06510.

0006-3495/94/03/654/13 $2.00

isoform resulted in loss of Cd^{2+} sensitivity and enhancement of TTX/STX sensitivity (Satin et al., 1992). Similarly, mutational substitution of the corresponding tyrosine residue in the skeletal muscle isoform to cysteine lowered the affinity for TTX/STX block and conferred high blocking affinity for Zn^{2+} and Cd^{2+} (Backx et al., 1992). Similar results were obtained for analogous experiments on the rat brain II sodium channel isoform that normally has phenylalanine in this position (Heinemann et al., 1992b). Thus, Cd^{2+} and Zn^{2+} are particularly useful probes of the ion conduction mechanism in cardiac sodium channels, since their binding site has been finely localized with the identification of cysteine 374 as a putative coordinating ligand for these metal ions.

From the voltage dependence of Cd^{2+} block in a cysteine-substituted mutant of the μ1 muscle sodium channel isoform, Backx et al. (1992) proposed that this cysteine residue is located within a β-sheet structure at a fractional electrical distance of 0.22 from the external side. By analogy to one widely considered structural model of the K^+ channel pore as a β-barrel (Durell and Guy, 1992), this location would place the cysteine group inside the narrow single-filing region of the sodium channel. However, this model is in apparent conflict with our previous finding that Zn^{2+} induces a subconductance state rather a complete block of Na^+ current through BTX-modified channels (Schild et al., 1991). The observation of a subconductance state implies that the Zn^{2+}-binding site cannot be located in the single-filing region of the pore, otherwise Na^+ current would be completely blocked when Zn^{2+} is bound. A Zn^{2+}-occupied substate is also relevant to the question of whether the Na^+ channel is a multi-ion pore (Begenisich, 1987), because it suggests that Na^+ can bind and permeate while some part of the channel, perhaps the outer vestibule, is simultaneously occupied by Zn^{2+}.

In this paper, we investigate the mechanism underlying the Zn^{2+}-induced subconductance state of BTX-modified sodium channels from heart by studying the current-voltage (I–V) behavior of both the open state and the Zn^{2+} substate over a wide range of symmetrical $[Na^+]$ as the only current carrier. The open state conductance of the cardiac sodium channel exhibits a biphasic dependence on $[Na^+]$ that is suggestive of a high and low affinity binding site for Na^+. This behavior is similar to that previously described for the skeletal muscle isoform (Ravindran et al., 1992). For the Zn^{2+}-occupied substate, we find that unitary conductance exhibits a monophasic dependence on $[Na^+]$ indicative of low affinity for Na^+. These observations can be explained by model in which the open channel functions as multi-ion pore that is subject to the effect of Na^+-Na^+ repulsion in the doubly occupied state. Zn^{2+} is proposed to bind to a site in the external vestibule such that it does not fully occlude entry to the single-filing region. Because of its close proximity to the pore, binding of a Zn^{2+} ion in this location would be expected to lower the affinity of the channel for Na^+ by a similar repulsive interaction between Zn^{2+} and Na^+. By this mechanism, the Zn^{2+}-occupied channel is practically limited to maximum occupancy by one Na^+ ion. Our results also place an important constraint on structural models of the sodium channel pore. They eliminate the possibility that the cysteine sulfhydryl group that coordinates Zn^{2+} is located exclusively within the narrow single-filing region of the channel.

MATERIALS AND METHODS

Planar bilayer recording

BTX-modified sodium channels from canine or bovine ventricular heart muscle were incorporated into planar lipid bilayers as previously described (Schild and Moczydlowski, 1991). Since cardiac sodium channels from these two species exhibit virtually indistinguishable unitary conductance and kinetics of block by saxitoxin and Zn^{2+} (Schild and Moczydlowski, 1991), data from both preparations were pooled for analysis. Bilayers were formed from a 4:1 mixture of bovine brain phosphatidylethanolamine:1,2-diphytanoylphosphatidylcholine (Avanti Polar Lipids, Birmingham, AL) in decane (25 mg/ml).

Single-channel current fluctuations were recorded at 21–24°C in the presence of symmetrical solutions containing 2.0 to 3006 mM Na^+ as the major inorganic cation. For NaCl concentrations ranging from 50 to 3000 mM, the buffer was 10 mM 3-(*N*-morpholino)propanesulfonic acid (MOPS) and 0.2 mM EDTA (free acid) adjusted to pH 7.4 by addition of 6 mM NaOH. In the range of 2 to 30 mM Na^+, the solution was 2 mM MOPS, 0.1 mM EDTA, 1.2 mM NaOH, pH 7.4, and either 0.8, 3.8, 8.8, 18.8, or 28.8 NaCl. Zn^{2+}-induced substate fluctuations were recorded in the presence of similar solutions containing 50 to 3006 mM NaCl, 10 mM MOPS, 6 mM NaOH, pH 7.4, and $ZnCl_2$ (20 to 1280 μM) as necessary to induce a convenient frequency of substate events (Schild et al., 1991).

Measurement of single-channel I–V curves. To ensure accurate recognition of open state and substate levels, unitary currents were measured from steady-state recordings (filtered at 20–200 Hz) of single-channels taken at 10-mV intervals over the voltage range of approximately −70 to +70 mV. For the open channel, the data set includes results from 3–11 bilayers at each of 12 symmetrical Na^+ concentrations ranging from 2 to 3006 mM. For the Zn^{2+} substate, similar data was obtained from three to five bilayers at each of six concentrations of Na^+ from 106 to 3006 mM. Unitary currents were measured as the difference between the closed state and the open state or the major substate observed upon addition of Zn^{2+} (Schild et al., 1991). Most of the recordings contained sufficient numbers of spontaneous closing events to provide accurate identification of the closed (zero-current) level; however, in some cases saxitoxin or decarbamoylsaxitoxin was used to induce discrete blocking events (Guo et al., 1987). For a given bilayer, each I–V point was determined as the mean of 5–10 current values. Applied voltages were corrected for a small junction potential (< 5 mV) as described previously (Ravindran et al., 1992). Current values were variously measured by three methods: directly from chart recordings using a digitizing tablet (Model TG1017; Houston Instuments), a measuring utility of the TAC program that employs a mouse-driven cursor (Instrutech Corp., Elmont, NY), or from peaks of amplitude histograms compiled with the aid of PCLAMP software (Axon Instuments, Foster City, CA). Current values measured by these three methods were statistically indistinguishable. To aid in measuring the peak maxima of all-points amplitude histograms such as those of Fig. 2, the histograms were fit with a sum of four Gaussian components using a utility of PCLAMP. Three of these Gaussian curves correspond to closed, open, and Zn^{2+} substate levels. A fourth broad Gaussian component was needed to smooth data resulting from rapid flickering between the open state and the Zn^{2+} substate (see Fig. 2).

Modeling of energy barrier profiles. I–V data collected at various Na^+ concentrations were fit to discrete-state barrier models of ion permeation with the use of the AJUSTE program described by Alvarez et al. (1992). Modeling of the open state energy profile of the BTX-modified cardiac sodium channel followed an approach similar to that used previously for a related sodium channel isoform from rat skeletal muscle (Ravindran et al., 1992). The model is based on a kinetic scheme for a 3-barrier-2-site (3B2S) channel that includes double-ion occupancy and Na^+-Na^+ repulsion. The

version of the model used here does not attempt to account for the effect of electrostatic surface potential due to the presence of fixed charges in the channel's vestibule (Green and Andersen, 1991; Latorre et al., 1992). Advantages and/or limitations of this approach and issues related to surface potential are considered under Discussion.

The model for the open state includes six adjustable energy parameters: three peak energies (G1, G2, G3), two wells or site energies (U1, U2), and one ion-ion repulsion parameter, A. The subscripts of the parameters refer to position with respect to the inside solution as shown in the upper diagram of Fig. 6. The effect of the repulsive interaction on the rate of Na^+ dissociation from or association to the doubly occupied state is modeled by addition of an energy, A/d, to peaks and wells adjacent to an occupied site, where d is the fractional electrical distance from the occupied site. The locations of peaks and wells are specified by six distance parameters, $D1$ through $D6$ as in Fig. 6 (*top*), which have dimensionless units of fractional electrical distance and sum to 1.0. The permeation model used to fit I–V data for the Zn^{2+}-induced substate was the same 3B2S model used for the open state except that the channel was effectively restricted to single occupancy by Na^+ by setting the Na^+-Na^+ repulsion parameter A, equal to 10RT.

Suitable D parameters were found by allowing the fitting routine to find simultaneous best-fit values of the six energy parameters at various arrangements of fixed D values. To limit the parameter search, D values were arbitrarily constrained by a requirement of symmetry about the central barrier located at an electrical distance of 0.5 according to: $D1 = D6$, $D2 = D5$, and $D3 = D4$. The quality of fits was evaluated both visually and by SUMSQ, which is the weighted sum of squared differences between experimental and theoretical data minimized by the fitting routine (Alvarez et al., 1992). The weighting factor, W, for each current value, I, was $W = |1/I|$ for $I > 0.1$ pA and $W = 10$ for $I \leq 0.1$ pA. This method of weighting enhances the fit to data points at low voltage which helps to identify models that predict the conductance behavior at 0 mV. As previously found for similar data collected for a sodium channel subtype from skeletal muscle (Ravindran et al., 1992), the optimum distance arrangement for the open state data was close to a uniform voltage dependence for each transition, i.e., all D values ~1/6. Best-fit values of the G and U parameters for the open state data were relatively insensitive to various arrangements of Ds, However, the value of repulsion parameter, A, is highly correlated with the particular arrangement of electrical distances since repulsion energy is calculated according to A/d, where d is the sum of D values from the occupied site to the adjacent site or outer barrier. In contrast to the rather ohmic I–V data for the open state, fitting of the weakly rectifying I–V data for the Zn^{2+} substate was more sensitive to values of the electrical distances for the various barriers. Empirically, we found that fits of the Zn^{2+} substate data did not converge for $U1$ when $D3$ and $D4$ were less than 0.2. The final partition of electrical distances chosen for the fits presented in Figs. 3–6 is: $D1 = D2 = D5 = D6 = 0.1$ and $D3 = D4 = 0.3$. This distance arrangement is not unique, but it allows convergence of both open state and Zn^{2+} substate I–V data to well-defined values for all the energy parameters. It also roughly matches electrical distances for the two wells estimated from the voltage dependence of external and internal block of BTX-modified sodium channels by various divalent cations and protons (Moczydlowski et al., 1986; Ravindran et al., 1991; Daumas and Andersen, 1993; French et al., 1994). In regard to the assumption of symmetrical D values, it is worth noting that distinct asymmetry previously observed for the blocking action of H^+ and Ca^{2+} implies that an asymmetrical barrier structure might be more realistic (Daumas and Andersen, 1993; French et al., 1994).

For the open state, conductance at zero voltage (see Fig. 5) was estimated from the slope conductance obtained by linear regression of I–V data in the range of ±50 mV. For the Zn^{2+} substate, conductance at zero voltage was estimated by nonlinear fitting of the weaky rectifying I–V data to the second order polynomial, $y = ax^2 + bx$, using the curve fit utility of Sigmaplot software (Jandel Corporation). The first derivative of this fit was used to obtain an estimate of conductance at 0 mV.

Single ion activities for Na^+ as calculated from solution activity coefficients were used for computations in the 3B2S model. The text and figures refer to total Na^+ concentration for ease of discussion. Following standard practice in applications of Eyring theory (Dani and Levitt, 1990), rate constants for ionic translocations assume a transmission coefficient of unity. Association rates are also divided by the molar concentration of water to convert to dimensionless mole fraction units (Eisenman and Dani, 1986). Our values of energy parameters are thus based on a solution reference state of 55.5 M. Conversion to a 1 M reference state is readily accomplished by addition of 4.0 RT units to the reported peak and well energies.

Measurement of Zn^{2+} rate constants. As previously described (Schild et al., 1991), Zn^{2+}-induced flickering events reflect binding and unbinding of Zn^{2+} to a site on the channel, but appear to be more complex than what is predicted by a simple one-step blocking process. However, within a certain range of $[Zn^{2+}]$ (~40–160 μM at 0.2 M NaCl) the mean dwell time of the Zn^{2+} substate events is independent of $[Zn^{2+}]$, and the mean open state dwell time between Zn^{2+} substates is inversely proportional to $[Zn^{2+}]$ as expected for a reversible binding reaction (Schild et al., 1991). To examine the effect of $[Na^+]$ on the kinetics of Zn^{2+} interaction with the channel, we recorded Zn^{2+}-induced flickering events using greater than 40 μM $ZnCl_2$ at +50 and −50 mV for symmetrical NaCl ranging from 50 to 3,000 mM. Single-channel dwell time histograms were compiled and analyzed as described previously (Schild et al., 1991). The apparent dissociation rate constant for Zn^{2+}, k_{off}, was taken to be the reciprocal lifetime of the component in the closed state histogram corresponding to dwell times of the Zn^{2+} substate. The apparent association rate constant for Zn^{2+} was taken to be the reciprocal lifetime of the monoexponential open state histogram with a small correction for missed closures (Schild et al., 1991). This latter value was converted to a bimolecular rate constant, k_{on}, by dividing by $[Zn^{2+}]$. The reported rate constants at 0 mV (see Fig. 7) were obtained by interpolating data at +50 and −50 mV with an exponential function of voltage.

RESULTS

Previously, we described characteristics of discrete flickering events induced by micromolar concentrations of external Zn^{2+} in single cardiac sodium channels modified by BTX (Schild et al., 1991). The Zn^{2+}-induced fickering events are not due to complete blockage of the channel. At 0.2 M symmetrical Na^+, they can be resolved as transitions to a low amplitude subconductance state that exhibits outwardly rectifying I–V behavior compared to the nearly ohmic I–V behavior of the open channel (Schild et al., 1991). Fig. 1 shows bilayer recordings of single BTX-modified Na^+channels from calf heart in the presence of external Zn^{2+} and symmetrical $[Na^+]$ ranging from 0.1 to 3.0 M. At −70 mV and 0.1 M Na^+ the brief Zn^{2+}-induced flickering events appear to close nearly to the zero-current level as recognized by comparison to longer duration closures of normal channel gating events. However, at +70 mV the non-zero level of the Zn^{2+}-induced substate at 0.1 M Na^+ can be clearly discerned (Fig. 1). At higher Na^+ concentrations, the substate current level can be recognized by a distinctive envelope of flicker transitions. As $[Na^+]$ is raised, the substate current progressively increases until it is roughly half the magnitude of the open channel at 3.0 M Na^+ (Fig. 1).

The mean current levels of closed, open, and subconductance states were measured by amplitude histograms such as those in Fig. 2. As described previously (Schild et al., 1991), titration of Zn^{2+} in the micromolar range at a fixed concentration of Na^+ increases the frequency of Zn^{2+}-induced flickering events but does not alter the mean current level of resolved dwell times in subconductance state. The results of Figs. 1 and 2 demonstrate that the Zn^{2+}-occupied state of the channel is poorly conductive at low Na^+ (< 100 mM), but it does conduct a substantial fraction of the open-state current

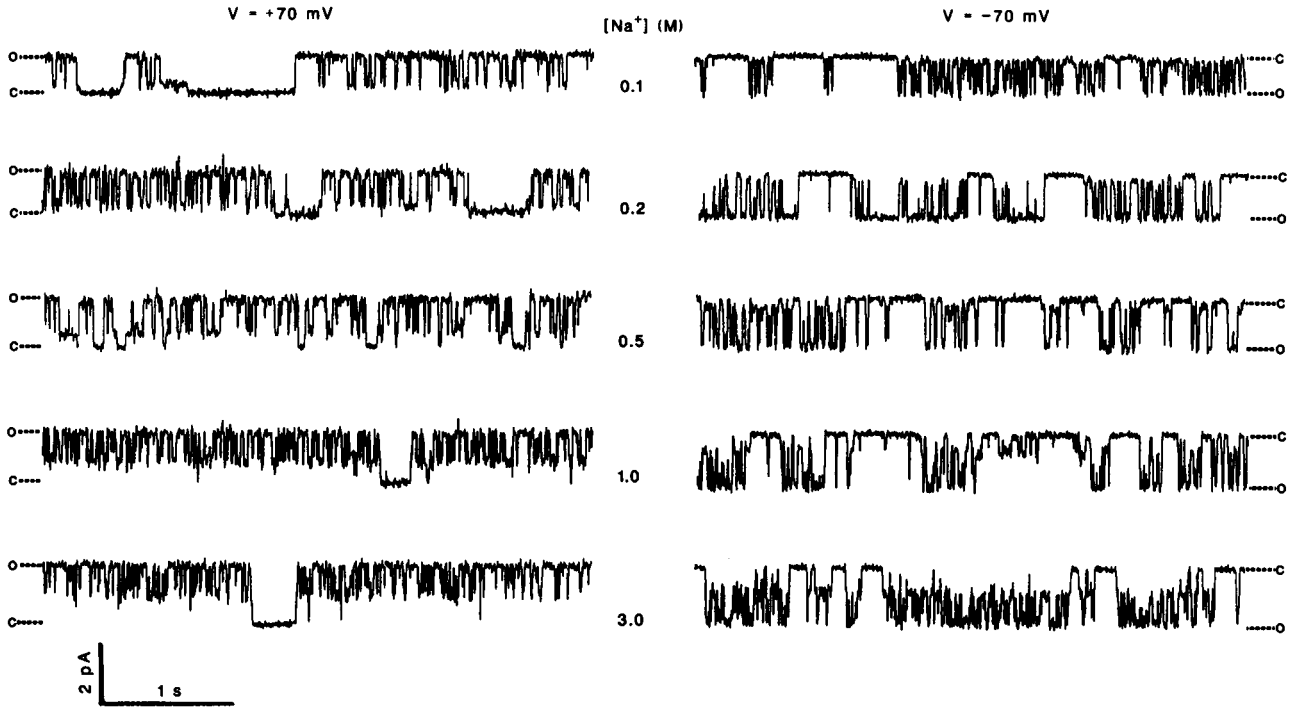

FIGURE 1 Current records of BTX-modified sodium channels from calf heart in the presence of external Zn^{2+}. Single sodium channels were inserted into planar bilayers in the presence of various symmetrical concentrations of NaCl from 0.1 to 3.0 M as indicated. External $ZnCl_2$ in the range of 20 to 640 μM was added to induce a convenient frequency of flickering events. Representative records taken at +70 or −70 mV are shown filtered at 100 Hz. Closed (*c*) and open (*o*) levels are indicated by dashed lines.

in the range of 1–3 M Na^+. Since the current-voltage (I–V) behavior of the Zn^{2+}-induced substate reflects an altered energy profile for Na^+ permeation, we analyzed this behavior in an attempt to determine how binding of a Zn^{2+} ion affects the energetics of Na^+ conduction through the channel.

Figs. 3 and 4 display I–V data at various Na^+ concentrations for the open and Zn^{2+}-occupied substate, respectively. As previously observed at 0.2 M Na^+ (Schild et al., 1991) open channel I–V curves are approximately linear, whereas the Zn^{2+} substate data follow weakly rectifying behavior; i.e., higher absolute current at positive versus negative voltage. To examine the dependence of unitary conductance on [Na^+] for the fully open state, a linear-regression fit of I–V data in the range of ± 50 mV was used to estimate the slope conductance at zero voltage. Similarly, I–V data for the Zn^{2+} substate were fit to a second-order polynomial (described in Materials and Methods), and the first derivative of this function was used to estimate conductance at 0 mV. Results of this analysis are shown in Fig. 5, where zero-voltage conductance versus [Na^+] for both states is plotted in log-log (Fig. 5 *A*) and linear (Fig. 5 *B*) format for comparison.

Like the skeletal muscle sodium channel characterized previously (Ravindran et al., 1992), the open state of the cardiac sodium channel has a relatively high conductance in the presence of symmetrical 2 mM Na^+ (11.1 ± 1.2 pS for heart vs. 8.0 ± 1.2 pS for muscle). In the range of 2 to 200 mM Na^+, the open-state conductance steeply increases from

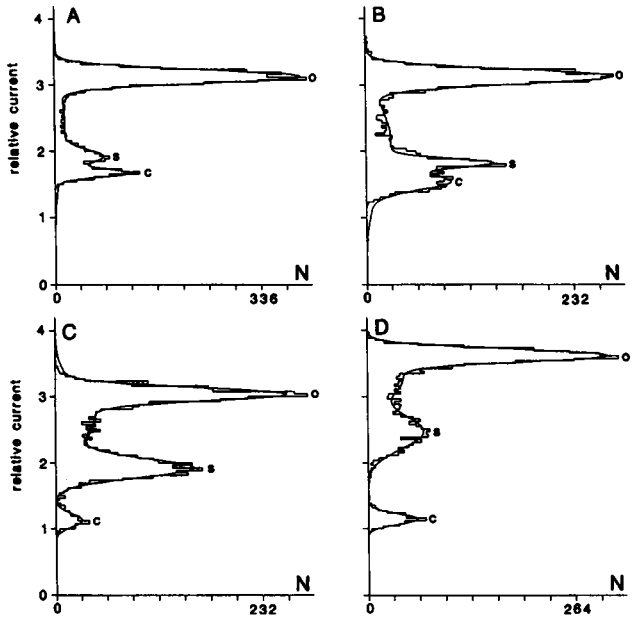

FIGURE 2 Current amplitude histograms from single sodium channels in the presence of external Zn^{2+}. Calf heart Na^+ channels were recorded at 100-Hz filtering as in Fig. 1. Data segments of 4.1 s in duration at +70 mV were digitized at 1 kHz and compiled into amplitude histograms at a resolution of 0.04 pA per bin. Relative current scale on the ordinate corresponds to 1.04 pA per division with the closed (*c*) level taken to be zero current. The abscissa is the number of points per bin (*N*). The symmetrical NaCl concentration was 0.1 M (*A*), 0.2 M (*B*), 1.0 M (*C*), or 3.0 M (*D*). Data were fit to a sum of four Gaussian components as described under Materials and Methods. Peaks correspond to closed (*c*), substate (*s*) and open (*o*) levels.

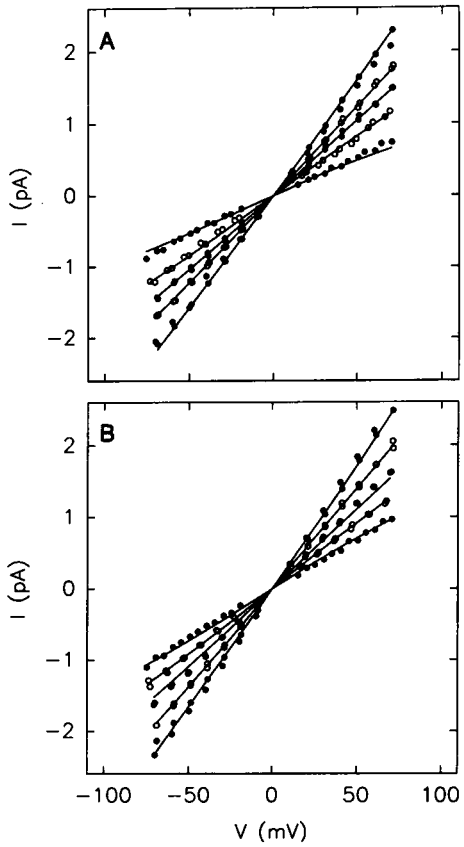

FIGURE 3 Current-voltage behavior of the open conductance state of BTX-modified sodium channels from calf heart. Data points are single-channel current-voltage measurements from two bilayers each at 10 different concentrations of Na^+. Current amplitudes were measured as the difference between open and closed current levels. Continuous lines are theoretical curves calculated from the 3B2S double-occupancy model of the open-state shown in Fig. 6. Data and curves of increasing slope correspond to the following concentrations of symmetrical Na^+ (mM): (*A*) 2, 10, 106, 506, and 2006; (*B*) 5, 20, 206, 1006, and 3006. Solid and open symbols are alternated for clarity.

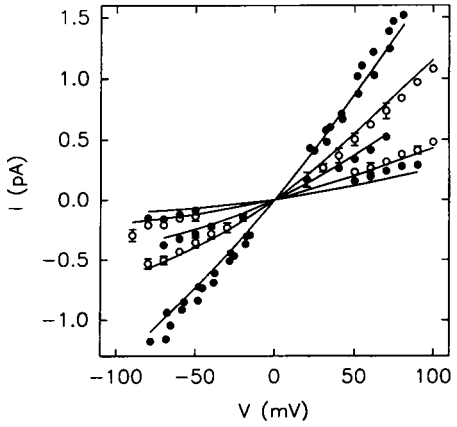

FIGURE 4 Current-voltage behavior of the Zn^{2+}-induced conductance substate of BTX-modified sodium channels from calf heart. Data points correspond to measurements of single-channel current of the Zn^{2+}-induced substate at five different concentrations of symmetrical Na^+. Current amplitudes were measured as the difference between the substate and the closed current level as described under Materials and Methods. Continuous lines are theoretical curves calculated from the 3B2S single-occupancy model of the Zn^{2+} substate shown in Fig. 6. Data and curves of increasing slope correspond to the following concentrations of symmetrical Na^+ (mM): 106, 206, 506, 1006, and 3006. Solid and open symbols are alternated for clarity.

11 to 23 pS, and then exhibits a more gradual rise to ~34 pS at 3000 mM Na^+ (Fig. 5 *B*). In contrast, measurable conductance of the Zn^{2+} substate can only be observed at ~100 mM Na^+, and it gradually increases to ~17 pS at 3,000 mM Na^+. Thus, the two conductance states of the cardiac sodium channel exhibit very different dependence on [Na^+]. Assuming that these two conductance states differ only by the presence of a bound Zn^{2+} ion, they can be used to assess the energetic impact of placing a divalent cation within a channel's vestibule. To interpret this behavior we sought to identify the simplest models of ion permeation compatible with these observations. For this application we employed reaction rate theory of ion permeation which describes the path of ion movement through the channel by an energy barrier profile (Andersen, 1989; Dani and Levitt, 1990; Alvarez et al., 1992).

In modeling the energy profile of the open state, we followed an approach previously used for the skeletal muscle sodium channel (Ravindran et al., 1992). In principle, a biphasic dependence of unitary conductance on [Na^+] can occur for a channel that simultaneously binds at least two ions and binds the second ion with lower affinity than the first (Hille and Schwarz, 1978). This situation may arise if the two Na^+ binding sites are located close enough to sense Na^+-Na^+ repulsion or if there is some other type of negative allosteric interaction between the two sites. A simple model incorporating these features is a 3-barrier-2-site (3B2S) kinetic scheme that permits double occupancy and includes a repulsion parameter as described under Materials and Methods. To test the ability of this model to describe the data, we performed simultaneous nonlinear least-square fitting of I–V data points collected at 12 concentrations of Na^+. For a given set of symmetrically arranged electrical distances (*D*1–*D*6, Fig. 6, *top diagram*), we found that the fitting program converged on well-defined values of peak and well energies that simulated the observed behavior. An example of such a fit is shown by the solid lines for the open state data in Figs. 3 and 5. Table 1 lists the values of the energy parameters for this fit, and Fig. 6 (open state) illustrates the corresponding energy profile.

The energy profile derived for the unoccupied open state (*solid line* in Fig. 6) is nearly symmetrical about the central peak and is quite similar to that previously described for a sodium channel isoform from rat skeletal muscle (Ravindran et al., 1992). For direct comparison, Table 1 includes the results of refitting the previously published I–V data for the skeletal muscle channel with the same distance parameters used here. Fig. 6 also compares the energy profile for the unoccupied channel (open state, *solid line*) with that of the doubly occupied channel (open state, *dotted line*) to illustrate the repulsive effect of bound Na^+. According to the model, the inverse dependence of the repulsive interaction on distance results in an increase in the energy barrier for asso-

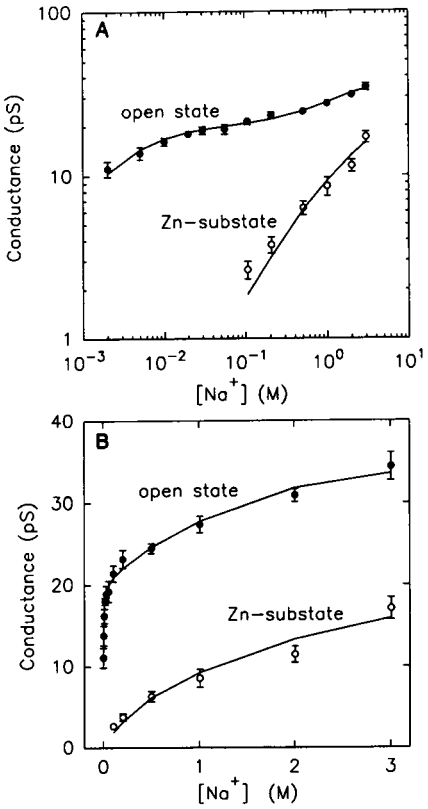

FIGURE 5 Conductance versus [Na^+] behavior of the open state and Zn^{2+}-induced substate of cardiac Na^+ channels modified by BTX. (*A*) Comparison of unitary conductance at 0 mV for both states plotted in log-log format. (*B*) Same data in *A* is shown on a linear scale for comparison. Solid lines connect theoretical points calculated for the respective energy barrier models shown in Fig. 6. Error bars refer to standard deviations larger than the symbol for data collected from three to 10 bilayers.

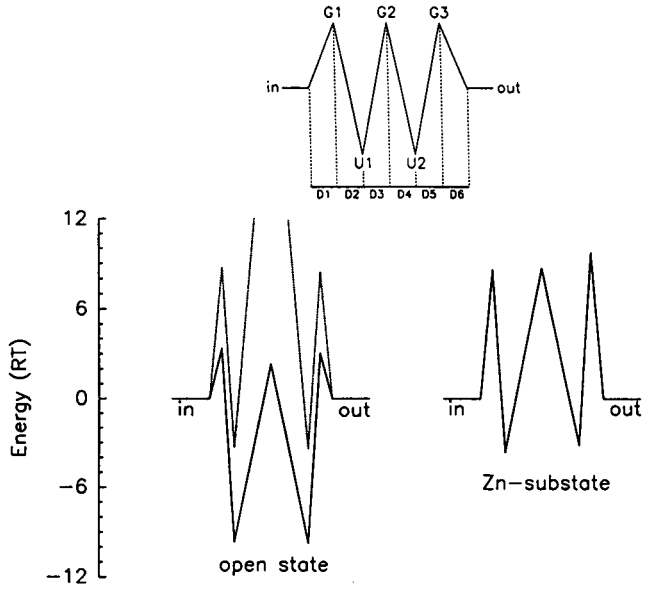

FIGURE 6 Energy barrier models of Na^+ permeation through the open state and Zn^{2+}-induced substate of cardiac sodium channels modified by BTX. Energy diagrams are drawn according to best-fit parameter values for a 3B2S model of Na^+ permeation listed in Table 1. The top diagram indicates parameters of the model: peak energies (*G*1–*G*3), well energies (*U*1, *U*2), and electrical distances (*D*1–*D*6). The open state model permits double occupancy by Na^+, whereas the model for the Zn^{2+} substate allows only single occupancy by Na^+. In the model of the open state, the solid line is the energy profile of the unoccupied channel and the dotted line is that of the doubly occupied channel to illustrate the effect of Na^+-Na^+ repulsion. In the doubly occupied state, the central peak is omitted to indicate single filing.

ciation of an ion from solution to the singly occupied state and a net decrease in the energy barrier for dissociation from the doubly occupied state to solution. From transition state theory, these effects correspond to a slower association rate constant and a faster dissociation rate constant for binding of a second Na^+ ion. At equilibrium, the effect of ion-ion repulsion is to lower the affinity of Na^+ binding to the singly occupied channel by a factor of ~560. Using a free energy reference state of 1.0 M and the relation, $\Delta G = RT\ln K_D$, the barrier model of the open state in Fig. 6 predicts equilibrium K_D values of Na^+ binding to the channel of ~3.4 mM and ~1900 mM for the unoccupied and occupied states, respectively.

In contrast to the biphasic dependence of zero-voltage conductance on [Na^+] observed for the open channel, the analogous relationship for the Zn^{2+} substate is monophasic within the limitations of experimental uncertainty (Fig. 5). As plotted in Fig. 5 *B* the conductance (g) versus [Na^+] relation for the Zn^{2+} substate is suggestive of a Michaelis-Menten relationship, $g = g_{max}[Na^+]/\{K_m + [Na^+]\}$, that would be predicted for a channel that can bind a maximum of one ion at a time (Läuger, 1973). In the context of barrier models, this observation lends itself to a rather simple interpretation.

TABLE 1 Comparison of best-fit energy parameters for a 3B2S model of Na^+ permeation through BTX-modified sodium channels of rat muscle, calf heart and a Zn^{2+}-occupied subconductance state of calf heart

Parameter	Muscle	Heart	Heart Zn^{2+} substate
*G*1	3.53 ± 0.05	3.37 ± 0.04	8.60 ± 0.19
*G*2	1.85 ± 0.09	2.32 ± 0.04	8.73 ± 0.54
*G*3	3.50 ± 0.05	3.04 ± 0.05	9.74 ± 0.11
*U*1	−9.69 ± 0.05	−9.64 ± 0.04	−3.63 ± 0.14
*U*2	−9.73 ± 0.05	−9.73 ± 0.03	−3.15 ± 0.12
A	3.34 ± 0.05	3.79 ± 0.03	10.0
SUMSQ	0.557	0.664	0.943

Single-channel I–V data at various concentrations of symmetrical Na^+ were fit to a 3B2S model of Na^+ permeation using the AJUSTE program (Alvarez et al., 1992) as described under Materials and Methods. Energy values are in *RT* units. Standard deviations derived from the fitting procedure are listed for parameters that were allowed to vary. For the case of the Zn^{2+} substate, the repulsion parameter, *A*, was fixed at 10*RT* to impose single-occupancy by Na^+. Distance parameters for these fits defined as in Fig. 6 (*top*) were fixed at $D1 = D2 = D5 = D6 = 0.1$ and $D3 = D4 = 0.3$. SUMSQ is the weighted sum of squared differences of experimental and theoretical data minimized in the fit (Alvarez et al., 1992).

Based on mutagenesis data (Satin et al., 1992; Backx et al, 1992; Schild et al., 1993), our interpretation assumes that Zn^{2+} binds within the outer vestibule of the channel at a location close to but not occluding the entrance to the single-filing region of the pore. In principle, the repulsive effect of a bound Zn^{2+} ion at this location would be similar to that

described above for the case of Na^+ binding to a channel already occupied by one Na^+ ion. Thus, we hypothesize that binding of Zn^{2+} in the vestibule raises the energy barrier profile for Na^+ permeation via Zn^{2+}-Na^+ repulsion and effectively limits the channel to single occupancy for Na^+ by greatly reducing the affinity for Na^+ binding to the Zn^{2+}-occupied channel.

To test whether this idea is applicable, we fit the combined I–V data for the Zn^{2+} substate at six different concentrations of symmetrical [Na^+] to a 3B2S barrier profile that was restricted to single occupancy by Na^+. An example of a best fit for a particular set of distance parameters is illustrated by the solid line curves in Fig. 4 and Fig. 5 for the Zn^{2+} substate. None of the fits that we obtained perfectly matched all of the individual I–V curves of Fig. 4. This seems to be related to random scatter in the data and errors associated with the measurement of very small current levels rather than a serious failure of the model. Table 1 lists the energy parameters for this fit, and Fig. 6 shows the corresponding energy profile. The profile produces weakly rectifying I–V behavior mainly by a higher entry barrier for inward versus outward Na^+ movement ($G3 > G1$). Compared to the unoccupied state of the open channel, the energy profile for the Zn^{2+} substate is characterized by higher peaks and shallower wells. In energetic terms, this means that it is more difficult for Na^+ to enter the channel in the Zn^{2+} substate; and, that the substate has a lower binding affinity for Na^+. According to a calculation similar to that described for the open channel, the two wells of the substate energy profile correspond to low affinity K_D values for Na^+ binding of ~1.5 M ($U1$) and ~2.4 M ($U2$). Inspection of the energy parameters in Table 1 indicates that on average, the peak and well energies derived for the Zn^{2+} substate are about 6 RT units higher than those of the open state. In the context of the model, binding of Zn^{2+} to a site in the vestibule introduces a replusive potential that effectively raises the whole profile by a constant amount of energy. The modeling results also suggest that the Zn^{2+} substate (Fig. 6) has an energy profile similar to that of the open state when doubly occupied by Na^+ (Fig. 6, open state, *dotted line*).

The conductance behavior described above addresses the effect of a bound Zn^{2+} ion on the permeation of Na^+. To view the problem from the opposite perspective, we also studied the effect of [Na^+] on the apparent rate constants for Zn^{2+} binding. As outlined previously (Schild et al., 1991), information on the kinetics of Zn^{2+} binding can be derived from dwell time analysis of Zn^{2+}-induced flickering. However, the kinetics of the Zn^{2+}-induced substate process are more complex than a simple reversible binding reaction, because the dwell time of the substate appears to depend on Zn^{2+} concentration (Schild et al., 1991). With this caveat, Fig. 7 shows apparent association (k_{on}) and dissociation (k_{off}) rate constants for Zn^{2+} (at 0 mV) as deduced from analysis of dwell time histograms of Zn^{2+}-induced flickering events collected at various concentrations of symmetrical [Na^+]. The observed k_{on} sharply declines from 50 to 500 mM Na^+ and appears to approach a constant value at higher Na^+. In

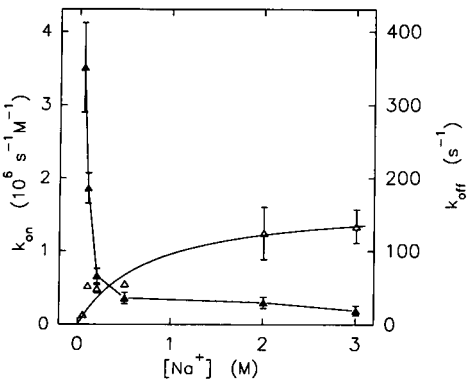

FIGURE 7 Dependence of Zn^{2+} kinetics on Na^+ concentration. Apparent association (k_{on},) and dissociation (k_{off}, Δ) rate constants for Zn^{2+} block at 0 mV were measured from Zn^{2+}-induced substate fluctuations over the range of 50 to 3000 mM NaCl as described under Materials and Methods. Error bars indicate the average of the relative standard deviation for data collected at +50 and −50 mV. Solid lines have no theoretical significance.

contrast, the observed k_{off} gradually increases with [Na^+] in a manner similar to that of the conductance of the Zn^{2+} substate shown in Fig. 5 *B*. These results are difficult to interpret quantitatively, because, in addition to kinetic complexity, ionic strength is not constant, leading to a large variation in surface potential. Nevertheless, we would argue that they are qualitatively compatible with our model of ion-ion interactions. As outlined under Discussion, the interactions between Zn^{2+} and Na^+ that we observe for the cardiac sodium channel are reminiscent of ion-ion interactions that have been described for voltage-dependent calcium channels (Tsien et al., 1987). In particular, the results of Fig. 7 can be compared to similar results observed for the effect of permeant [Ba^{2+}] on the rate constant for Cd^{2+} block in the calcium channel (Fig. 4 of Lansman et al. (1986)).

Similar to the interpretation of Lansman et al. (1986) in the latter case, the effect of [Na^+] on the dissociation of Zn^{2+} reflects binding of Na^+ to a Zn^{2+}-occupied channel and the increase in the k_{off} of Zn^{2+} in Fig. 7 is due to Zn^{2+}-Na^+ repulsion. This interaction occurs with an apparent low affinity for Na^+ (K_d ~1 M) similar to that observed for permeation of Na^+ through the Zn^{2+} substate (Fig. 5). The effect of [Na^+] on association of Zn^{2+} may be interpreted as strong competition between Zn^{2+} and Na^+ for binding to the unoccupied channel. According the barrier model of Fig. 6, the unoccupied channel has a relatively high affinity for Na^+ (K_D ~3 mM) and this appears to be reflected in a large decrease in the k_{on} of Zn^{2+} in the region less than 0.2 M Na^+. As Na^+ saturates its high affinity site, the k_{on} of Zn^{2+} falls precipitously. This effect is anticipated, since the conductance data of Fig. 5 implies that binding of Zn^{2+} eliminates high affinity binding of Na^+, and Na^+ should therefore inhibit binding of Zn^{2+}.

To provide a structural basis for this apparent binding competition, we propose that the high affinity site for Na^+ is very close to the Zn^{2+} site in the external vestibule. This is compatible with independent information from studies of the TTX/STX binding reaction. From blocking/binding com-

petition studies (Schild and Moczydlowski, 1991; Doyle et al., 1993) and from site-directed mutagenesis experiments (Backx et al., 1992; Schild et al., 1993), it appears that the high affinity Zn^{2+}-binding site of cardiac Na^+ channels overlaps the STX-binding site in the external vestibule. Studies of [^{3}H]STX binding at constant ionic strength (~600 mM) have also shown that there is direct binding competition between STX and Na^+ with an apparent K_d for Na^+ of ~30 mM (Weigele and Barchi, 1978; Barchi and Weigele, 1979). These overlapping, three-way, competitive relationships between Zn^{2+}-STX, Na^+-STX, and Zn^{2+}-Na^+ reinforce the suggestion that the Zn^{2+}-binding site is in close proximity to a site that binds Na^+ in the unoccupied channel with an apparent K_d in the mM range.

To summarize, the conductance data of Fig. 5 and the kinetic data of Fig. 7 are consistent with the existence of high and low affinity sites for Na^+ that participate in the conduction process. Based on binding competition studies cited above, the high affinity site for Na^+ appears to overlap or be located very near the external Zn^{2+} binding site. Low affinity binding of Na^+ is proposed to arise from direct ion-ion repulsion. Functional expression of low affinity for Na^+ is observed when one Na^+ ion is bound to the open channel or when Zn^{2+} is bound to a subconductance state of the channel.

DISCUSSION

Utility of Eyring energy barrier models

This study describes the conductance behavior of the open state and a Zn^{2+}-induced substate of cardiac sodium channels modified by BTX. Analysis of the mechanism of substate production must consider that conduction of ions through channel proteins consists of three basic processes: diffusion of an ion up to the entrance of the pore, dehydration and solvation of the ion by polar chemical groups, and translocation across energy barriers (Andersen and Koeppe, 1992). Binding of Zn^{2+} to a site in the vestibule of the cardiac sodium channel could affect conduction of Na^+ by perturbing any or all of these steps. *A priori*, bound Zn^{2+} may be expected to perturb Na^+ diffusion near the pore entrance by reducing negative surface potential that tends to concentrate Na^+. Depending on proximity, Zn^{2+} could perturb binding of Na^+ to sites in the channel by directly interfering with ligand coordination or indirectly by ion-ion repulsion. Zn^{2+} binding could also allosterically perturb the conformational dynamics of pore residues and thus alter "fluctuating barrier" processes that may involved in ion translocation (Läuger et al., 1980). Given our incomplete understanding of these important molecular details, it is clear that a computational or modeling approach to the present data is unlikely to yield a unique description of the Zn^{2+} substate.

To facilitate interpretation, we have fit the I–V data to discrete-state models of Na^+ permeation formulated in terms of energy barrier profiles and Eyring transition state theory. As discussed by various authors (Cooper et al., 1988; Dani and Levitt, 1990), quantitative application of this approach to channel proteins has certain theoretical limitations and is not expected to provide a physically accurate representation of the conduction pathway. Nevertheless, the method is valuable for determining whether conductance data are consistent with particular permeation mechanisms. In this context, our barrier model is a minimalistic scheme that focuses on the role of ion-ion interactions in multi-ion channels. This emphasis was chosen because the present findings combined with results of recent mutagenesis experiments (Backx et al., 1992; Heinemann et al., 1992a, b; Satin et al., 1992; Schild et al., 1993) allow an attractive argument to be made for functional similarities between sodium and calcium channels. Before discussing this analogy, we consider how the effect of vestibule surface charge may affect our interpretation.

Surface electrostatics versus direct ion-ion interactions

In sodium channels, the existence of negative surface potential in the extracellular vestibule has been inferred from many results including studies of the relative association rates of the guanidinium toxins, STX^{2+} and TTX^{1+} as a function of [NaCl] (Green et al., 1987; Ravindran and Moczydlowski, 1989). Negative surface charges located in channel vestibules have been proposed to enhance conduction by increasing the local concentration of permeant cations available for flux through the pore (Green and Andersen, 1991; Latorre et al., 1992). The electric field associated with vestibule surface charge has also been proposed to act by superposition upon the energy profile for ion conduction, in effect, by tilting the profile to affect rate limiting steps of ion movement (MacKinnon et al., 1989). The effect of surface charge on Na^+ permeation through BTX-modified sodium channels has been previously modeled using Gouy-Chapman theory for a planar charge distribution (Green et al., 1987b; Correa et al., 1991; Naranjo and Latorre, 1993) and by numerical solution of the Poisson-Boltzmann equation for various geometries and charge distributions chosen to emulate the mouth of a channel protein (Cai and Jordan, 1990). These studies have shown that fixed negative surface charges can theoretically lead to a large increase in local Na^+ concentration near pore entrances, particularly at low ionic strength. Such models have the common property that surface potential is screened by counterions and is effectively diminished at high ionic strength.

This characteristic dependence of surface potential on ionic strength may be used to infer that the Zn^{2+} substate is not solely a surface charge effect caused by partial neutralization of negative charges by Zn^{2+}. The data of Fig. 5 indicates that the conductance of the Zn^{2+} substate is 50% of the open state conductance at 3.0 M NaCl. At this high ionic strength, both the Gouy-Chapman theory (Green and Andersen, 1991; Latorre et al., 1992) and theories based on a more realistic geometry (Dani, 1986; Cai and Jordan, 1990) predict that surface charge effects on conductance should be minimal if not negligible. If the Zn^{2+} substate were simply the result of surface charge neutralization, one would expect

the substate conductance to closely approach that of the open state above ~1.0 M NaCl. The fact that there is still a twofold difference in conductance at 3.0 M NaCl (Fig. 5) strongly suggests that other mechanisms are involved, such as direct effects of Zn^{2+} on Na^+ binding.

A consideration of the number of charges likely to contribute to the external electrostatic field in the Na^+ channel also suggests that a net change of +2 electronic charges due to binding of Zn^{2+} is macroscopically negligible. For example, it has been estimated that there are approximately 100 negatively charged sialic acid residues on the carbohydrate chains attached to the extracellular domain of the *Electrophorus* sodium channel (Miller et al., 1983). In terms of charged amino acid residues, the folding model of Numa and Noda (1986) predicts that there are 24 basic residues (Lys + Arg) and 41 acidic residues (Asp + Glu) within the four S5–S6 extracellular linker regions of domains I–IV of the rat brain II sodium channel. If surface potential effects result from the smeared distribution of a large number of charged groups on the protein and/or carbohydrate, then a change of +2 would be insignificant. If, on the other hand, surface charge effects on conductance are primarily mediated by a few charged groups at a specific location such as the pore entrance, then a change of +2 charges could have a profound effect.

An indication of the influence of charged amino acid residues on sodium channel conductance can be obtained from the work of Terlau et al. (1991) who examined the effect of charge changes in the S5–S6 linker domains (I–IV) on TTX/STX sensitivity and single-channel conductance in the rat brain II isoform. Although some of the charge change mutations that affected TTX/STX sensitivity also reduced conductance, there were numerous exceptions. By plotting all of their data as conductance versus change of charge from wild type, we found a poor correlation between these two parameters ($r = -0.45$). In particular, none of the mutations that increased net negative charge resulted in an increase in conductance that would be expected if negative surface charge were a primary determinant of Na^+ flux at physiological ionic strength. Instead of indicating a general long-range effect of negative surface charge, the data of Terlau et al. (1991) and Heinemann et al. (1992b) are more consistent with the notion that specific charged residues participate in the conduction process via direct binding interactions with permeant ions and divalent cations.

These considerations lead us to propose that the Zn^{2+} substate is primarily due to perturbation of Na^+ binding and translocation via ion-ion interactions as implied by the energy barrier model described under Results. However, our data does not rule against the possibility that negative surface charge enhances unitary conductance of the open state at very low ionic strength. Also, we cannot eliminate the possibility that the low conductance of the Zn^{2+} substate at low [Na^+] (less than ~200 mM) is partly due to reduction in local [Na^+] via surface electrostatics.

The Zn^{2+}-Na^+ interaction recalls features of permeation through Ca^{2+} channels

As shown here (Fig. 3) and elsewhere (Garber, 1988; Correa et al., 1991; Ravindran et al., 1992; Naranjo and Latorre, 1993), sodium channels display nearly linear I–V behavior over a wide range of symmetrical [Na^+] that is suggestive of a symmetric energy profile. In general, divalent cations permeate poorly through sodium channels if at all (Yamamoto et al., 1984; Nilius, 1988). Rather, various divalent cations block sodium channels both extracellularly (Ravindran et al., 1991) and intracellularly (Albitz et al, 1990; Lin et al., 1991; French et al., 1994) under conditions of symmetrical Na^+. In the simplest interpretation, the voltage dependence observed for these respective blocking reactions implies that there are two divalent cation blocking sites each located at a fractional electrical distance of ~0.2 from each end of the channel.

Studies of calcium channel permeation have led to a similar picture. In the absence of divalent cations, Na^+ permeation through calcium channels is characterized by a nearly linear I–V curve with a unitary conductance of ~90 pS at 0.2 M symmetrical NaCl (Rosenberg and Chen, 1991). Low concentrations of divalent cations block Na^+ current through calcium channels from both the extracellular and intracellular sides. Single-channel analysis of Ca^{2+} block of Na^+ current suggests that the pore of L-type calcium channels has two high affinity sites (K_d ~2 μM) for Ca^{2+} located at ~0.15 and ~0.85 fractional electrical distance (Rosenberg and Chen, 1991). Thus, from a functional perspective, Na^+ current carried by sodium channels and calcium channels is similar with respect to block by divalent cations. The major difference concerns selectivity: calcium channels have micromolar affinity for Ca^{2+} and other divalent cations which permeate, while sodium channels have millimolar affinity for divalent cations that permeate poorly if at all. Functional similarity of the blocking reactions for these two channels is not unanticipated, given the high degree of primary sequence homology of sodium and calcium channels within the superfamily of voltage-gated channels (Numa et al., 1986; Tanabe et al., 1987).

Key observations regarding ion permeation through calcium channels have been explained on the basis of a 3B2S double-occupancy model of conduction (Almers and McCleskey, 1984; Hess and Tsien, 1984). Ca^{2+} current through calcium channels is thought to arise from a destabilizing or repulsive interaction between the two Ca^{2+} sites. Double occupancy by Ca^{2+} is presumed to destabilize high affinity binding of Ca^{2+} to the unoccupied channel. This destabilization enhances the rate of Ca^{2+} dissociation and produces measurable Ca^{2+} current. Aside from results of this paper, previous evidence for multi-ion occupancy in sodium channels is strong but ambiguous. Concentration-dependent permeability ratios have been used to infer multiple occupancy in sodium channels (Begenisich, 1987; Yamamoto et al., 1985), but under special circumstances, models of

single-occupancy pores can also exhibit such behavior (Eisenman and Horn, 1983). Flux ratio exponents (n') significantly greater than 1.0 have been measured for Na^+ channels (Busath and Begenisich, 1982); however, such behavior can apparently arise in single-occupancy channels if there is barrier asymmetry for two different ions (Busath and Begenisich, 1982). Also, the biphasic dependence of open state conductance on [Na^+] (Fig. 5), that we have suggested to be a consequence of double occupancy (Ravindran et al., 1992), can be mimicked by various models of surface charge coupled to a one-site channel (Dani, 1986; Cai and Jordan, 1990; Latorre et al. 1992). Thus, the observation of Na^+ current through the Zn^{2+} substate is significant, because it suggests that the ion conduction pathway of the cardiac sodium channel, defined as two vestibules connected by a narrow pore, can be simultaneously occupied by Zn^{2+} and Na^+.

This Zn^{2+}-Na^+ co-occupancy and the functional similarities between calcium and sodium channels motivates application of a 3B2S conduction model to cardiac sodium channels and allows us to compare permeation through these two channels within the same theoretical framework. Our modeling results support the idea that the unoccupied sodium channel has a lower intrinsic affinity in the millimolar range for its natural substrate, Na^+, than that of calcium channels which effectively bind Ca^{2+} in the micromolar range. The barrier model of the open state (Fig. 6) is in basic agreement with previous conclusions (Begenisich and Busath, 1981), that the sodium channel is primarily singly occupied by Na^+ in physiological solutions ([Na^+] ~100 mM). However, as noted above, the second rising phase of current observed at higher [Na^+] (Fig. 5) can be interpreted as a propensity for double occupancy. Our conductance data and modeling results suggest that the Zn^{2+}-bound channel emulates the low affinity state of the open channel for Na^+ that is postulated to occur via repulsion.

In considering the mechanism of the Zn^{2+} substate, it is important to note that there is no evidence to indicate that Zn^{2+} permeates through the channel. We have not observed enhancement of current by millimolar Zn^{2+} or shifts of reversal potential that would demonstrate measureable current carried by external Zn^{2+} (Ravindran et al., 1991). Also, Zn^{2+} does not appear to induce substate events when added to the intracellular side of the channel (L. Schild and E. Moczydlowski, unpublished observations). This suggests that Zn^{2+} cannot easily reach its external high-affinity site by passing through the channel from the inside. The observed voltage dependence of Zn^{2+} binding to its external high-affinity site is consistent with a location that is ~0.20–0.23 of the fractional electrical distance from the outside (Schild et al., 1991). This is virtually the same electrical distance as that found for other divalent cations that block sodium channels from the extracellular side (Ravindran et al., 1991). How can the Zn^{2+} site be located at an electrical distance of ~0.20 of the electric field, not fully block or occlude the channel, and yet exert a profound effect on Na^+ conduction? The available evidence suggests that the high-affinity Zn^{2+} site lies within a wide external antechamber or vestibule leading to the narrow tunnel where the movement of ions is restricted to single-file. Furthermore, the Zn^{2+} site must be close enough to the entrance of this tunnel to exert a repulsive influence on Na^+ ions entering from either side. This location is compatible with an analysis of channel electrostatics which concludes that the influence of transmembrane voltage can extend across part of a channel's two vestibules as well as the narrow single-filing region (Jordan, 1986). Theoretical calculations of bulk electrostatics for an hourglass geometry typically assumed for a channel protein suggest that a large fraction (~30%) of the potential drop across such a structure may fall within the vestibule (Jordan, 1986).

Although placement of the Zn^{2+}-binding site in the outer vestibule most economically addresses our results, it does disagree with some attempts to draw direct structural analogies between oligomeric K^+ channels and pseudo-oligomeric sodium channels. Based on sequence analysis and mutagenesis of K^+ channels, Durrel and Guy (1992) have proposed that a particular "P-region" segment of the S5–S6 linker region of *Drosophila* K^+ channels forms an eight-stranded β-barrel that composes the K^+-selective pore. In suggesting a structure for the sodium channel pore region fashioned according to Durrell and Guy (1992), two groups (Backx et al., 1992; Doyle et al., 1993) have proposed models of the β-hairpin that would place the cysteine group required for Zn^{2+}/Cd^{2+} binding within the narrowest region of the pore. This location would predict a complete blockage of the channel by Zn^{2+} rather than a subconductance state. Since these proposals cannot be comfortably reconciled with our results on Na^+ conductance of the Zn^{2+} substate, we favor an approach to modeling the structure of the sodium and calcium channel pore region that relies on direct functional analysis of these two channels rather than a comparison with more distantly related K^+ channels.

Structural basis for ion selectivity and block by external divalent cations in calcium and sodium channels

Recent mutagenesis experiments on various sodium channel isoforms expressed in *Xenopus* oocytes have identified particular residues in the S5–S6 linker region that strongly affect binding and selectivity for divalent cations. One line of investigation identified a cysteine residue (Cys^{374}) in the cardiac subtype that accounts for the unique sensitivity of this sodium channel isoform to group IIB metals such as Cd^{2+} and Zn^{2+} (Satin et al., 1992; Backx et al., 1992). A second line of investigation identified a position (one residue away from Cys^{374}) in the alignment of the S5–S6 linker region which consists of four glutamate residues in calcium channels and contains aspartate(I), glutamate(II), lysine(III), and alanine(IV) in the respective I–IV internally homologous domains of sodium channels (Heinemann et al., 1992b). The conversion of the lysine(III) or alanine(IV) residues to glutamate resulted in selectivity properties characteristic of cal-

cium channels such as block of Na^+ current by micromolar Ca^{2+} and actual permeation by Ca^{2+} in the millimolar range (Heinemann et al., 1992b). These latter experiments indicate that this position is a key determinant of selectivity for monovalent versus divalent cations. With the assumption that the aqueous channel is formed by a cavity at the interface of domains I–IV, the results of Heinemann et al. (1992) suggest that a high-affinity binding site for Ca^{2+} is formed by the simultaneous participation of three or four acidic residues (glutamate or aspartate) in the outer well. This finding is reminiscent of Ca^{2+}-binding sites in protein structures that have been identified by x-ray crystallography. Such sites usually contain three to five carboxylate groups of aspartate or glutamate residues as direct ligands of Ca^{2+} (Quiocho et al., 1987; Nakayama et al., 1992). Thus in Fig. 8 we propose a schematic version of the external Ca^{2+} binding site

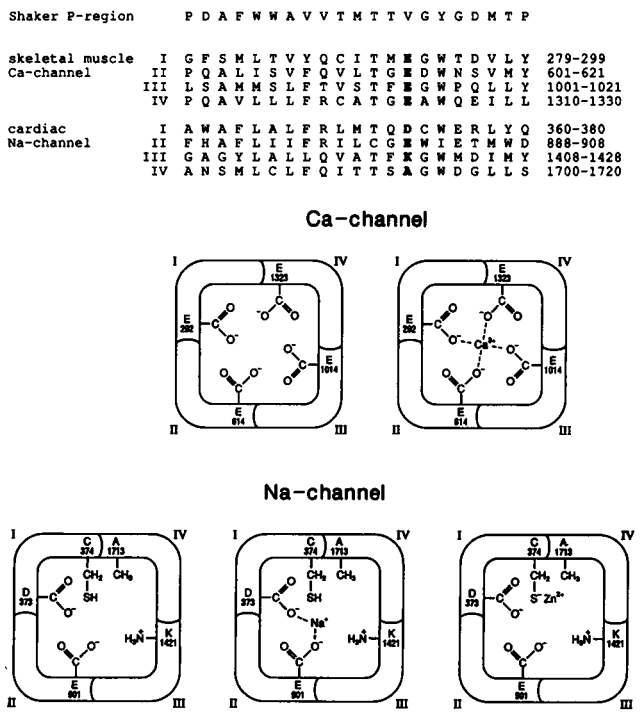

FIGURE 8 Schematic models of external cation binding sites in calcium and sodium channels. The upper sequence alignment (after Guy and Conti, 1990) shows the S5–S6 linker region of a *Drosophila* Shaker K^+ channel identified as forming part of the channel pore (Yellen et al., 1991). The K^+ channel P-region is aligned with four corresponding domains of a skeletal muscle calcium channel (Tanabe et al., 1987) and a rat cardiac sodium channel (Rogart et al., 1989). The aligned residues in bold type are represented in the lower diagrams and are proposed to participate in cation selectivity and block by external divalent cations in calcium and sodium channels (Heinemann et al., 1992b). Residues depicted for the calcium channel correspond to four aligned glutamate residues (E292, E614, E1014, E1323) in domains I–IV. The left and right diagrams for the calcium channel correspond to the unoccupied and Ca^{2+}-bound states, respectively. Residues for the cardiac sodium channel correspond to aligned aspartate(D373), glutamate(E901), lysine(K1421), and alanine(A1713) residues in domains I–IV, respectively. The cysteine residue (C374 in domain I) implicated in high affinity block of the cardiac sodium channels by Cd^{2+} and Zn^{2+} (Satin et al., 1992; Backx et al., 1992) is also shown. The left, center and right diagrams for the sodium channel correspond to unoccupied, Na^+-occupied and Zn^{2+}-occupied states, respectively.

of calcium channels formed by carboxylate groups of the four aligned glutamates residues identified by Heinemann et al. (1992b). With respect to a typically assumed hourglass-shaped conduction pathway, Fig. 8 is intended to represent a thin slice of structure in the outer vestibule of the channel that is located just at the entrance to the narrow region of the pore: In the absence of Ca^{2+}, this site could bind Na^+ weakly and allow the calcium channel to conduct Na^+ current. However, in the presence of micromolar Ca^{2+}, tight binding of this divalent cation to this site would completely block Na^+ current.

The bottom panel of Fig. 8 shows the analogous version of the outer site proposed for the cardiac sodium channel. The four glutamate residues in the calcium channel are replaced by the functional groups of aspartate(I), glutamate(II), lysine(III), and alanine(IV) in the respective (I–IV) internally homologous domains. This structure allows external Ca^{2+} to completely block Na^+ current by coordinating with the carboxyl groups of aspartate(I) and glutamate(II), but the affinity for external Ca^{2+} is lowered to the millimolar range by energetic destabilization resulting from substitution of glutamate (III and IV) in calcium channels with the functional groups of the lysine(III) and alanine(IV) residues in sodium channels. In accord with the results of Heinemann et al. (1992b), this model ascribes an important function of the lysine(III) and alanine(IV) residues at the outer well of sodium channels: allowing for the preferential permeation of monovalent versus divalent cations by reducing the affinity for Ca^{2+}. This scheme can also account for the Zn^{2+} substate (Fig. 8, *right bottom*). The sulfhydryl group of cysteine 374 is proposed to be close to the entrance to the pore and serve as a major coordinating ligand for Zn^{2+}. At this location, Zn^{2+} does not prevent entry of Na^+ into the pore, but it greatly reduces the affinity for Na^+ by direct repulsion and/or steric hinderance.

This scheme accounts for the known interactions of monovalent and divalent cations at the external entrance of calcium and sodium channels, but it does not specify the structural basis for double occupancy by permeant ions that is an important feature of the 3B2S energy barrier description. As one possibility, a second Ca^{2+}/Na^+ site could be formed by a different region of the protein such as the S4–S5 intracellular linker domain identified by Isacoff et al. (1991) as forming part of the inner vestibule of K^+ channels. Alternatively, it is possible that double occupancy by permeant ions takes place in close proximity to the region shown in Fig. 8. Armstrong and Neyton (1991) have proposed a permeation model involving a local cluster of carboxylate groups that binds two Ca^{2+} ions. This latter model mimics the general properties of the 3B2S description of calcium channels. It can be generated by modifying the schematic diagram of Fig. 8 to allow the adjacent binding of two Ca^{2+} ions as discussed in a recent study of calcium channel permeation (Yang et al., 1993). In conclusion, a comparison of the permeation behavior of sodium and calcium channels can be used to design a structural model of the external ion binding site of these two

channels that qualitatively explains divalent versus monovalent cation selectivity and accounts for the Zn^{2+} substate.

We thank Dr. Arippa Ravindran for his participation in the conductance measurements and Ivan Gautschi for excellent technical assistance. We also thank Drs. George Eisenman and Osvaldo Alvarez for helpful discussions on modeling strategy for sharing their AJUSTE computer program.
This work was supported by grants from the Swiss National Science Foundation (to L. S.) and the National Institues of Health (to E. M.).

REFERENCES

Albitz, R., J. Magyar, and B. Nilius. 1990. Block of single cardiac sodium channels by intracellular magnesium. *Eur. Biophys. J.* 19:19–23.

Almers, W., and E. W. McCleskey. 1984. Non-selective conductance in calcium channels of frog muscle: calcium selectivity in a single-file pore. *J. Physiol. (Lond.)*. 353:585–608.

Alvarez, O., A. Villarroel, and G. Eisenman. 1992. Calculation of ion currents from energy profiles and energy profiles from ion currents in multibarrier, multisite, multioccupancy channel model. *Meth. Enzymol.* 207: 816–854.

Andersen, O. S. 1989. Kinetics of ion movements mediated by carriers and channels. *Meth. Enzymol.* 171:62–112.

Andersen, O. S., and R. E. Koeppe. 1992. Molecular determinants of channel function. *Physiol. Rev.* 72:S89-S158.

Armstrong, C. M., and J. Neyton. 1991. Ion permeation through calcium channels. A one-site model. *Ann. NY Acad. Sci.* 653:18–25.

Backx, P. H., D. T. Yue, J. H. Lawrence, E. Marban, and G. F. Tomaselli. 1992. Molecular localization of an ion-binding site within the pore of mammalian sodium channels. *Science (Wash. DC)*. 257:248–251.

Barchi, R. L., and J. B. Weigele. 1979. Characteristics of saxitoxin binding to the sodium channel of sarcolemma isolated from rat skeletal muscle. *J. Physiol. (Lond.)*. 295:383–396.

Begenisich, 1987. Molecular properties of ion permeation through sodium channels. *Ann. Rev. Biophys. Biophys. Chem.* 16:247–263.

Begenisich, T., and D. Busath. 1981. Sodium flux ratio in voltage-clamped squid giant axons. *J. Gen. Physiol.* 77:489–502.

Behrens, M. I., A. Oberhauser, F. Bezanilla, and R. Latorre. 1989. Batrachotoxin-modified sodium channels from squid optic nerve in planar bilayers. Ion conduction and gating properties. *J. Gen. Physiol.* 93:23–41.

Busath, D., and Begenisich, T. 1982. Unidirectional sodium and potassium fluxes through the sodium channel of squid giant axons. *Biophys. J.* 40: 41–49.

Cooper, K. E., P. Y. Gates, and R. S. Eisenberg. 1988. Diffusion theory and discrete rate constants in ion permeation. *J. Membr. Biol.* 106:95–105.

Cai, M., and P. C. Jordan. 1990. How does vestibule surface charge affect ion conduction and toxin binding in a sodium channel? *Biophys. J.* 57: 883–891.

Correa, A. M., R. Latorre, and F. Bezanilla. 1991. Ion permeation in normal and batrachotoxin-modified Na^+ channels in the squid giant axon. *J. Gen. Physiol.* 97:605–625.

Dani, J. A. 1986. Ion-channel entrances influence permeation. Net charge, size, shape, and binding considerations. *Biophys. J.* 49:607–618.

Dani, J. A., and D. G. Levitt. 1990. Diffusion and kinetic approaches to describe permeation in ionic channels. *J. Theor. Biol.* 146:289–301.

Daumas, P., and O. S. Andersen. 1993. Proton block of rat brain sodium channels. Evidence for two proton binding sites and multiple occupancy. *J. Gen. Physiol.* 101:27–43.

Doyle, D. D., Y. Guo, S. L. Lustig, J. Satin, R. B. Rogart, and H. A. Fozzard. 1993. Divalent cation competition with [^{3}H]saxitoxin binding to tetrodotoxin-resistant and -sensitive sodium channels. A two-site structural model of ion/toxin interaction. *J. Gen. Physiol.* 101:153–182.

Durell, S. R., and H. R. Guy. 1992. Atomic scale structure and functional models of voltage-gated potassium channels. *Biophys. J.* 62:238–250.

Eisenman, G., and J. A. Dani. 1986. Characterizing the electrical behavior of an open channel via the energy profile for ion permeation. A prototype using a fluctuating barrier model for the acetylcholine receptor. *In* Ionic Channels in Cells and Model Systems. R. Latorre, editor. Plenum Press, New York. 53–87.

Eisenman, G., and R. Horn. 1983. Ionic selectivity revisited: the role of kinetic and equilibrium processes in ion permeation through channels. *J. Membrn. Biol.* 76:197–225.

French, R. J., J. F. Worley, W. F. Wonderlin, A. S. Kularatna, and B. K. Krueger. 1994. Ion permeation, divalent ion block and chemical modification of single sodium channels: description by single- and double-occupancy rate-theory model. *J. Gen. Physiol.* In press.

Garber, S. S. 1988. Symmetry and asymmetry of permeation through toxin-modified Na^+ channels. *Biophys. J.* 54:767–776.

Green, W. N., and O. S. Andersen. 1991. Surface charges and ion channel function. *Annu. Rev. Physiol.* 53:341–359.

Green, W. N., L. B. Weiss, and O. S. Andersen. 1987a. Batrachotoxin-modified sodium channels in planar lipid bilayers. Ion permeation and block. *J. Gen. Physiol.* 89:841–872.

Green, W. N., L. B. Weiss, and O. S. Andersen. 1987b. Batrachotoxin-modified sodium channels in planar lipid bilayers. Characterization of saxitoxin- and tetrodotoxin-induced channel closures. *J. Gen. Physiol.* 89:873–903.

Guo, X., A. Uehara, A. Ravindran, S. H. Bryant, S. Hall, and E. Moczydlowski. 1987. Kinetic basis for insensitivity to tetrodotoxin and saxitoxin in sodium channels of canine heart and denervated rat skeletal muscle. *Biochemistry*. 26:7546–7556.

Guy, H. R., and F. Conti. 1990. Pursuing the structure and function of voltage-gated channels. *Trends Neurosci.* 13:201–206.

Heinemann, S. H., H. Terlau, and K. Imoto. 1992a. Molecular basis for pharmacological differences between brain and cardiac sodium channels. *Pflügers. Arch.* 422:90–92.

Heinemann, S. H., H. Terlau, Stühmer, K. Imoto, and S. Numa. 1992b. Calcium channel characteristics conferred on the sodium channel by single mutations. *Nature (Lond.)*. 356:441–443.

Hess, P., and Tsien, R. W. 1984. Mechanism of ion permeation through calcium channels. *Nature (Lond.)*. 309:453–456.

Hille, B. 1975. The receptor for tetrodotoxin and saxitoxin: A structural hypothesis. *Biophys. J.* 15:615–619.

Hille, B., and W. Schwarz. 1978. Potassium channels as multi-ion single-file pores. *J. Gen. Physiol.* 72:409–442.

Isacoff, E. Y., Y. N. Jan, and L. Y. Jan. 1991. Putative receptor for the cytoplasmic inactivation gate in the *Shaker* K+ channel. *Nature (Lond.)* 353:86–90.

Jordan, P. C. 1986. Ion channel electrostatics and the shapes of channel proteins. *In* Ion Channel Reconstitution. C. Miller, editor. Plenum Press, New York. 37–55.

Lansman, J. B., P. Hess, and R. W. Tsien. 1986. Blockade of current through single calcium channels by Cd^{2+}, Mg^{2+}, and Ca^{2+}. Voltage and concentration dependence of calcium entry into the pore. *J. Gen. Physiol.* 88:321–347.

Latorre, R., P. Labarca, and D. Naranjo. 1992. Surface charge effects on ion conduction in ion channels. *Meth. Enzymol.* 207:471–501.

Läuger, P. 1973. Ion transport through pores: a rate theory analysis. *Biochim. Biophys. Acta.* 311:423–441.

Läuger, P., W. Stephan, and E. Frehland. 1980. Fluctuations of barrier structure in ionic channels. *Biochim. Biophys. Acta.* 602:167–180.

Lin, F., F. Conti, and O. Moran. 1991. Competitive blockage of the sodium channel by intracellular magnesium ions in central mammalian neurones. *Eur. Biophys. J.* 19:109–118.

MacKinnon, R., and C. Miller. 1989. Functional modification of a Ca^{2+}-activated K^+ channel by trimethyloxonium. *Biochemistry.* 28:8087–8092.

Miller, J. A., W. S. Agnew, and S. R. Levinson. 1983. Principal glycopeptide of the tetrodotoxin/saxitoxin binding protein from *Electrophorus electricus*: isolation and partial chemical and physical characterization. *Biochemistry.* 22:426–470.

Moczydlowski, E., A. Uehara, X. Guo, and J. Heiny. 1986. Isochannels and blocking modes of voltage-dependent sodium channels. *Ann. NY Acad. Sci.* 479:269–292.

Nakayama, S., N. D. Moncrief, and R. H. Kretsinger. 1992. Evolution of EF-hand calcium modulated protein. II. Domains of several subfamilies have diverse evolutionary histories. *J. Mol. Evol.* 34:416–448.

Naranjo, D., and R. Latorre. 1993. Ion conduction in substates of the batrachotoxin-modified Na^+ channel from toad skeletal muscle. *Biophys. J.* 64:1038–1050.

Nilius, B. 1988. calcium block of guinea-pig heart sodium channels with and without modification by the piperazinylindole DPI 201-106. *J. Physiol. (Lond.)*. 399:537–558.

Noda, M., H. Suzuki, S. Numa, and W. Stühmer. 1989. A single point mutation confers tetrodotoxin and saxitoxin insensitivity on sodium channel II. *FEBS Lett.* 259:213–216.

Numa, S., and M. Noda. 1986. Molecular structure of sodium channels. *Ann. NY Acad. Sci.* 479:338–355.

Quiocho, F. A., N. K. Vyas, J. S. Sack, and M. N. Vyas. 1987. Atomic protein structures reveal basic features of binding of sugars and ionic substrates, and calcium cation. *Cold Spring Harbor Symp. Quant. Biol.* 52:453–463.

Ravindran, A., and Moczydlowski, E. 1989. Influence of negative surface charge on toxin binding to canine heart Na channels in planar bilayers. *Biophys. J.* 55:359–365.

Ravindran, A., H. Kwiecinski, O. Alvarez, G. Eisenman, and E. Moczydlowski. 1992. Modeling ion permeation through batrachotoxin-modified Na^+ channels from rat skeletal muscle with a multi-ion pore. *Biophys. J.* 61:494–508.

Ravindran, A., L. Schild, and E. Moczydlowski. 1991. Divalent cation selectivity for external block of voltage-dependent Na^+ channels prolonged by batrachotoxin. Zn^{2+} induces discrete substates in cardiac Na^+ channels. *J. Gen. Physiol.* 97:89–115.

Rogart, R. B., L. L. Cribs, L. K. Muglia, D. D. Kephart, and M. W. Kaiser. 1989. Molecular cloning of a putative tetrodotoxin-resistant rat heart Na^+ channel isoform. *Proc. Natl. Acad. Sci. USA*. 86:8170–8174.

Rosenberg, R. L., and X. Chen. 1991. Characterization and localization of two ion-binding sites within the pore of cardiac L-type calcium channels. *J. Gen. Physiol.* 97:1207–1225.

Satin, J., J. W. Kyle, M. Chen, P. Bell, L. L. Cribbs, H. A. Fozzard, and R. B. Rogart. 1992. A mutant of TTX-resistant cardiac sodium channels with TTX-sensitive properties. *Science (Wash. DC)*. 256:1202–1205.

Schild, L., I. Favre, and E. Moczydlowski. 1993. Mechanism of zinc block in Na-channel subtypes and mutants. *Biophys. J.* 64:A4.

Schild, L., and E. Moczydlowski. 1991. Competitive binding interaction between Zn^{2+} and saxitoxin in cardiac Na^+ channels. Evidence for a sulfhydryl group in the Zn^{2+}/saxitoxin binding site. *Biophys. J.* 59: 523–537.

Schild, L., A. Ravindran, and E. Moczydlowski. 1991. Zn^{2+}-induced subconductance events in cardiac Na^+ channels prolonged by batrachotoxin. Current-voltage behavior and single-channel kinetics. *J. Gen. Physiol.* 97:117–142.

Tanabe, T., H. Takeshima, A. Mikami, V. Flockerzi, H. Takahashi, K. Kangawa, M. Kojima, H. Matsuo, T. Hirose, and S. Numa. 1987. Primary structure of the receptor for calcium channel blockers from skeletal muscle. *Nature (Lond.)*. 328:313–318.

Terlau, H., S. H. Heinemann, W. Stühmer, M. Pusch, F. Conti, K. Imoto, and S. Numa. 1991. Mapping the site of block by tetrodotoxin and saxitoxin of sodium channel II. *FEBS Lett.* 293:93–96.

Tsien, R. W., P. Hess, E. W. McCleskey, and R. L. Rosenberg. 1987. Calcium channels: mechanisms of selectivity, permeation and block. *Ann. Rev. Biophys. Biophys. Chem.* 16:265–290.

Weigele, J. B., and R. L. Barchi. 1978. Saxitoxin binding to the mammalian sodium channel. Competition by monovalent and divalent cations. *FEBS Lett.* 95:49–53.

Yamamoto, D., and J. Z. Yeh, and T. Narahashi. 1985. Interactions of permeant cations with sodium channels of squid axon membranes. *Biophys. J.* 48:361–368.

Yang, J., P. T. Ellinor, W. A. Sather, J.-F. Zhang, and R. W. Tsien. 1993. Molecular determinants of Ca^{2+} selectivity and ion permeation in L-type Ca^{2+} channels. *Nature (Lond.)*. 366:158–161.

Yellen, G., M. E. Jurman, T. Abramson, and R. MacKinnon. 1991. Mutations affecting internal TEA blockade identify the probable pore-forming region of a K^+ channel. *Science (Wash. DC)*. 251:939–944.